

Electrochemical and Photophysical Properties of a Series of Group-14 Metalloles

Justin Ferman,[‡] Joseph P. Kakareka,[§] Wim T. Klooster,^{||} Jerome L. Mullin,⁺
Joseph Quattrucci,[†] John S. Ricci,[†] Henry J. Tracy,^{*,†} William J. Vining,[‡] and Scott Wallace[†]

Department of Chemistry, University of Southern Maine, Portland, Maine, Department of Chemistry, University of Massachusetts, Amherst, Massachusetts, College of Arts and Sciences, Florida Gulf Coast University, Ft. Myers, Florida, Chemistry Department, Brookhaven National Laboratory, Upton, New York, and Department of Life Sciences, University of New England, Biddeford, Maine

Received June 11, 1998

A series of six group-14 dimethyl- or diphenyl-tetraphenylmetallacyclopentadienes were synthesized and characterized by their spectroscopic and electrochemical properties. The group-14 elements investigated were silicon, germanium, and tin. (The compounds are designated according to the heteroatom and the substituent on the heteroatom, i.e., SiMe, SiPh, ..., SnPh.) Five of the six compounds luminesce in both the solid state and in solution. The emission maxima of SiPh, GePh, and SnPh are invariant to a change in the heteroatom, while for SiMe, GeMe, and SnMe there is a strong dependence of the emission maxima on the identity of the heteroatom. SiMe emits at a longer wavelength than GeMe, while SnMe is not luminescent. The dramatic luminescence difference between the two tin compounds was investigated. ¹³C NMR coupling to ^{119/117}Sn, observed in both SnMe and SnPh, was used to make ¹³C NMR resonance assignments. Qualitative results of semiempirical molecular orbital calculations support the ¹³C NMR assignments. The crystal structure data for SnPh was obtained at 20 °C: *a* = 10.353(2) Å, *b* = 16.679(2) Å, *c* = 9.482(1) Å, α = 99.91(1)°, β = 106.33(1)°, γ = 77.80(1)° with *Z* = 2 in space group *P*₁. It is proposed that the increased electron density at tin in SnMe is responsible for the deactivation of the emissive state. The presence of phenyl substituents in SnPh serves to stabilize the emissive state and luminescence is observed.

Introduction

Group-14 and group-15 metalloles, five-membered metallacyclopentadienes (Figure 1), were first prepared by Braye and Leavitt in the early 1960s.^{1–3} In a recent review of the group-14 metalloles, Dubac has cataloged their syntheses, organic reaction chemistry, and some of their physical and chemical properties.⁴ Interest in this class of compounds has been motivated by the possibility of using metalloles as monomers for the preparation of conjugated polymers with very small band gaps that exhibit intrinsic conductivity or semiconducting properties.⁵ Our interest in this class of compounds was stimulated by the luminescent properties of several of the group-14 metalloles. Braye⁶ noted a strong blue fluorescence in ultraviolet light with hexaphenylsilole (SiPh), and Gilman⁷ noted a similar blue fluorescence with 1,1-dimethyl-2,3,4,5-tetraphenylsilole (SiMe). A brief comparison of the luminescence properties of some of the group-15 perphenylmetalloles has been published.⁸ Luminescence emission for pentaphenylpyrrole,

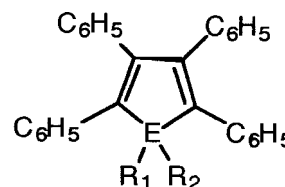


Figure 1. The general structure of metalloles. For group-14 metalloles, E = Si, Ge, Sn and R₁ = R₂ = Me or Ph. For group-15 metalloles, E = N, P, As and R₁ = Ph and R₂ is not present.

pentaphenylphosphole, and pentaphenylarsole (E = N, P, As, and R₁ = Ph in Figure 1) occurred at 487 ± 5 nm (with excitation at 320 nm). The identity of the heteroatom did not significantly affect the observed luminescence. No similar luminescence analyses of the group-14 metalloles have appeared.

In this paper we present a comparison of the photophysical and electrochemical properties of the methyl- and phenyl-substituted group-14 metalloles. For simplicity, these group-14 tetraphenylmetalloles will be referred to by their heteroatom and heteroatom substituent: SiMe, SiPh, GeMe, GePh, SnMe, and SnPh. We have attempted to interpret the experimental results by examining semiempirical molecular orbital calculations of these metalloles. A high-level *ab initio* calculation performed on a model compound supports the molecular orbital description obtained at the semiempirical level.

The metalloles were prepared from the dilithium reagent generated by the reductive coupling of diphenylacetylene in the presence of lithium metal as pioneered by Braye.⁴ The improvements to the original preparation noted by Eisch were em-

(8) Braye, E. H.; Raciszewski, Z. *Photochem. Photobiol.* **1970**, *12*, 429.

[†] University of Southern Maine.

[‡] University of Massachusetts.

[§] Florida Gulf Coast University.

^{||} Brookhaven National Laboratory.

⁺ University of New England.

(1) Braye, E. H.; Hubel, W.; Caplier, I. *J. Am. Chem. Soc.* **1961**, *83*, 4406.

(2) Leavitt, F. C.; Manuel, T. A.; Johnson, F. *J. Am. Chem. Soc.* **1959**, *81*, 3163.

(3) Leavitt, F. C.; Manuel, T. A.; Johnson, F.; Matternas, U.; Lehman, D. S. *J. Am. Chem. Soc.* **1960**, *82*, 5099.

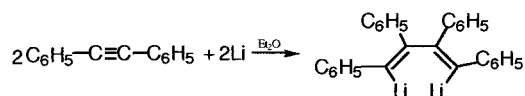
(4) Dubac, J.; Laporterie, A.; Manuel, G. *Chem. Rev.* **1990**, *90*, 215.

(5) Marynick, D. S.; Hong, S. Y. *Macromolecules* **1995**, *28*, 4991.

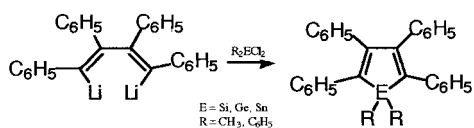
(6) Braye, E. H.; Hubel, W.; Caplier, I. *J. Am. Chem. Soc.* **1961**, *83*, 4406.

(7) Gilman, H.; Cottis, S. G.; Atwell, W. H. *J. Am. Chem. Soc.* **1964**, *86*, 1596.

Scheme 1



Scheme 2



ployed.⁹ The dilithium reagent, 1,4-dilithio-2,3,4,5-tetraphenylbutadiene, was then quenched with the appropriate dialkyl (or diaryl) dichlorides of silicon, germanium, or tin (Schemes 1 and 2). In the case of GePh, 1,1-dichloro-2,3,4,5-tetraphenylgermacyclopentadiene was prepared first and then phenyllithium was employed to synthesize the desired GePh. The metalloles were isolated by column chromatography on silica and purified by recrystallization. The six metalloles studied are yellow or pale yellow-green air-stable solids with melting points of 172–187 °C. All display a similar absorption band at approximately 350 nm that we attribute to the tetraphenyldiene section of the metallole.¹⁰ It is postulated, based on simple Hückel theory for *cis*-1,3-butadiene, that the shape of the highest occupied molecular orbital (HOMO) would be of a π -type symmetry localized at each of the formal carbon–carbon double bonds in the metallole. The lowest unoccupied molecular orbital (LUMO) would be predicted to have π^* -type symmetry with respect to the carbon–carbon double bonds. The planar structure of a simplified model metallole, hydrogen-substituted silole, and the surfaces of the HOMO and LUMO are displayed in Figure 2. Five of the six compounds are luminescent. The absorption, emission, mass, and nuclear magnetic resonance spectra and the cyclic voltammograms of these six metalloles were collected.

These metalloles all have planar metallacyclopentadiene moieties. The phenyl substituents on the diene have dihedral angles that vary from nearly 0° to a more expected 90° from the metallacyclopentadiene plane. The X-ray crystal structures of SiMe and GeMe have been published.^{11,12} Here we report the structure of hexaphenylstannole (SnPh). In solution, a low barrier to rotation for the phenyl substituents would be expected, although, due to steric repulsions, no two adjacent phenyl rings could be coplanar with the metallacyclopentadiene. The substituent-phenyl groups give the molecule a propeller-like shape.

Experimental Section

A. Materials. All synthetic experiments were carried out in a dry nitrogen or argon atmosphere using standard Schlenk techniques. Diethyl ether and tetrahydrofuran (THF) were dried over sodium/benzophenone ketyl and distilled before use. Dimethyldichlorosilane (Hüls) and diphenyldichlorosilane (Aldrich or Hüls) were distilled prior to use and stored over magnesium chips. Germanium(IV) chloride and diphenyltin dichloride were obtained from Alfa and used as received. Dimethyltin dichloride was sublimed in vacuo (0.05 mmHg, 25 °C) before use. Phenyllithium (Aldrich) and methylolithium (Fisher) were used as received. Column chromatography was performed over 60–200 mesh silica (Aldrich). Melting points are uncorrected.

(9) Eisch, J. J.; King, R. B. *Organometallic Synthesis*; Academic Press: NY, 1965; Vol 2, p 98.

(10) The two colorless byproducts of the syntheses, (*E,E*)-1,2,3,4-tetraphenylbuta-1,3-diene and (1,2,3,4-tetraphenylbuta-1,3-dienyl)dimethyltin chloride, both lack the metallole ring.

(11) For SiMe see: Parkanyi, L. *J. Organomet. Chem.* **1981**, 216, 9.

(12) For GeMe see: Meier-Brocks, F.; Weiss, E. *J. Organomet. Chem.* **1993**, 453, 33.

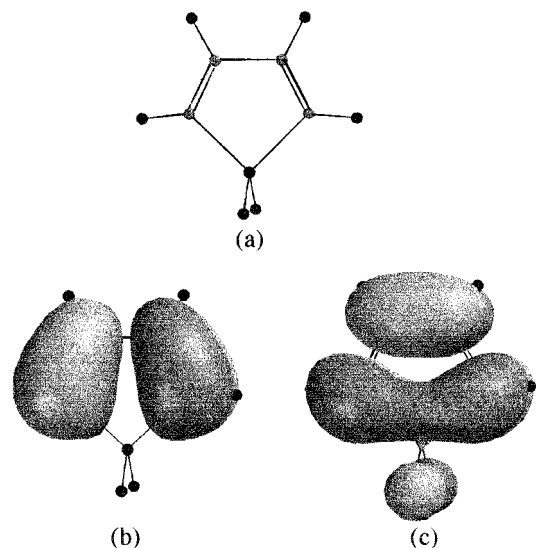


Figure 2. Structure of a metallole (a) and the isopotential surfaces of the HOMO (b) and LUMO (c) generated with MacSpartan at the ab initio level of theory (3-21G* level) of nonsubstituted silole ($\text{H}_2\text{SiC}_4\text{H}_4$).

B. Preparation of Compounds. In a typical reaction, 55 mmol (10 g) of diphenylacetylene, dried in vacuo overnight, was dissolved in 75 mL of diethyl ether and cannulated into a dry 500-mL three-necked round-bottom flask attached to a Schlenk line. Under a positive pressure of inert gas, lithium wire (55 mmol) that had been washed in hexanes was cut into 2–5-mm pieces into the reaction flask. Within 20–30 min of stirring, the reaction mixture became dark red. Stirring was continued for approximately 4 h, at which time the unreacted lithium wire was removed from the reaction mixture. The reaction mixture was stirred for an additional 1–2 h, but not longer than 16 h. (Longer reaction times can lead to the ring closure product, 2,3,4-triphenyl-1-naphthyllithium.⁷) At this point either of two procedures was followed: THF (100 mL) was added to the mixture and stirring was continued for several hours before aliquots of the reagent were hydrolyzed and titrated to determine the lithium reagent concentration. Alternatively, a cleaner lithium reagent can be obtained, if before the addition of THF, the reaction mixture is filtered and the yellow dilithio reagent precipitate is washed with dry hexane (3 × 20 mL) and then dissolved in dry THF (100 mL). In either case, a stoichiometric quantity of the (*E,E*)-1,2,3,4-tetraphenyl-1,3-butadiene-1,4-ylidenedilithium solution was then added, by syringe, to a stirred solution of the group-14 dihalide (or, in the case of GePh, the tetrahalide) in either diethyl ether or THF. The dimethyl dichlorides tended to react immediately, while the diphenyl dichlorides were slower to react. In either case, the lightening of the solution from dark blue-green (in THF solvent) to yellow or amber indicated that the metallole had been formed. The workup and isolation of the products followed one of two paths: Either a hydrolytic extraction was performed, or the ethers were removed from the reaction mixtures and the residue extracted with methylene chloride. In general, once a crude product was obtained either it was recrystallized or a portion of the product was subjected to column chromatography over 60–200 mesh silica. The diphenylacetylene starting material was eluted with petroleum ether or hexanes. The product metalloles were then eluted with a solvent system of approximately 40% methylene chloride and 60% petroleum ether. Further recrystallization in boiling ethanol, 2-propanol, or hexanes yielded purified products.

1. Synthesis of 1,1-Dimethyl-2,3,4,5-tetraphenylsilacyclopentadiene (SiMe).⁷ The standard reaction sequence was followed as described above using 10.1 g of diphenylacetylene (56.9 mmol) and 405 mg of lithium wire (58.4 mmol). After determining the concentration of the dilithio reagent by titration (14 mmol, 47% yield), the entire lithium reagent solution was quenched with 2.1 mL dimethyldichlorosilane (17 mmol). The solution lightened to yellow over the course of 30 min. The solvents were removed and the residue was extracted with methylene chloride. Concentration of the methylene chloride solution and precipitation by the addition of 2-propanol yielded 3.52 g

(8.5 mmol) of the crude silole (62% yield based on dilithio reagent). Recrystallization from 2-propanol yielded pure SiMe (52% yield based on crude).

SiMe: yellow-green solid; mp 182 °C. Elem. Anal. Calcd for $\text{SiC}_{30}\text{H}_{26}$: C, 86.91; H, 6.32. Found: C, 86.90; H, 6.39. UV-vis ($\text{CH}_3\text{-CN}$, nm): 351 ($3.2 \times 10^3 \text{ M}^{-1}\text{cm}^{-1}$). IR (KBr, cm^{-1}): 3077 (m), 3057 (m), 3022 (w), 2958 (w), 2898 (w), 1594 (m), 1572 (w), 1489 (m), 1440 (m), 1296 (m), 1244 (m), 1087 (w), 1074 (w), 1029 (m), 937 (m), 911 (m), 835 (m), 794 (s), 779 (s), 695 (s). EI-MS (70 V): major fragments at $m/z = 105, 221$, and molecular ion at $m/z = 414$. $^1\text{H NMR}$ (300 MHz, CDCl_3): δ 7.14–6.78 (m, 20H, C_6H_5), 0.47 (s, 6H, CH_3). $^{13}\text{C NMR}$ (75 MHz, CDCl_3): δ 153.91, 141.77, 139.83, 138.76, 129.97, 128.81, 127.90, 127.36, 126.15, 125.48, -3.90. CV: oxidation at 1450, 1750 mV vs Ag/AgCl, reduction at -2250 mV vs Ag/AgCl. Luminescence (acetonitrile): excitation at 351 nm, emission at 480 nm.

2. Synthesis of 1,1,2,3,4,5-Hexaphenylsilylacyclopentadiene (SiPh).¹ The standard reaction sequence was followed as described above using 10.4 g of diphenylacetylene (58.4 mmol) and 405 mg of lithium wire (58.4 mmol). The dilithio reagent was quenched with 6.1 mL of diphenyldichlorosilane (29 mmol) dissolved in 100 mL of THF. The diethyl ether was distilled off and the reaction solution was refluxed for an additional 4.5 h. When the reaction mixture had cooled, the solution was yellow-green. After hydrolytic workup and removal of the solvents, the metallole was isolated by column chromatography and purified by recrystallization from 2-propanol (3.28 g, 44% yield based on a 50% yield of dilithio reagent).

SiPh: yellow-green solid; mp 192–193 °C. Elem. Anal. Calcd for $\text{SiC}_{40}\text{H}_{30}$: C, 89.17; H, 5.61. Found: C, 89.09; H, 5.66. UV-vis ($\text{CH}_3\text{-CN}$, nm): 360 ($8.5 \times 10^3 \text{ M}^{-1}\text{cm}^{-1}$). IR (KBr, cm^{-1}): 3062 (m), 3021 (m), 1596 (m), 1571 (w), 1483 (m), 1441 (m), 1428 (m), 1110 (m), 1075 (w), 1027 (w), 935 (m), 916 (m), 790 (s), 762 (s), 740 (s), 714 (s), 695 (s), 529 (m). EI-MS (70 V): major fragments at $m/z = 105, 181, 193, 283$, and molecular ion at $m/z = 538$. $^1\text{H NMR}$ (300 MHz, CDCl_3): δ 7.68–7.34 (m, 10H, C_6H_5), 7.03–6.86 (m, 20H, C_6H_5). $^{13}\text{C NMR}$ (75 MHz, CDCl_3): δ 156.72, 139.56, 139.50, 138.76, 131.58, 130.12, 129.96, 129.20, 128.23, 127.75, 127.42, 126.36, 125.62. CV: oxidation at 1527, 1750 mV vs Ag/AgCl, reduction at -1943, -2116 mV vs Ag/AgCl. Luminescence (acetonitrile): excitation at 360 nm, emission at 496 nm.

3. Synthesis of 1,1-Dimethyl-2,3,4,5-tetraphenylgermacyclopentadiene (GeMe).¹² The standard reaction sequence was followed as described above to prepare the dilithio reagent using 20.1 g of diphenylacetylene (114 mmol) and 792 mg of lithium wire (114 mmol). A portion of the dilithio reagent (96 mL, 7.1 mmol) was quenched with 2.0 g of dimethylgermanium dichloride (12 mmol) dissolved in 30 mL of THF. An immediate color change occurred. The ethers were removed in vacuo and the crude product was extracted with methylene chloride. Concentration of the methylene chloride solution yielded 2.6 g (5.7 mmol, 81% based on dilithio reagent) of yellow-green crystals of GeMe. The germole was purified by recrystallization from ethanol/methylene chloride (51% yield based on crude).

GeMe: yellow-green solid; mp 178–180 °C. Elem. Anal. Calcd for $\text{GeC}_{30}\text{H}_{26}$: C, 78.48; H, 5.71. Found: C, 78.82; H, 5.58. UV-vis ($\text{CH}_3\text{-CN}$, nm): 348 ($3.8 \times 10^3 \text{ M}^{-1}\text{cm}^{-1}$). IR (KBr, cm^{-1}): 3075 (w), 3055 (m), 3019 (m), 2976 (w), 2906 (w), 1594 (m), 1571 (w), 1486 (m), 1440 (m), 1293 (w), 1267 (w), 1074 (w), 1028 (w), 912 (m), 830 (w), 786 (m), 763 (m), 738 (m), 706 (s), 695 (s), 562 (m). EI-MS (70 V): major fragments at $m/z = 89, 151, 178, 267, 356$, and molecular ion at $m/z = 460$. $^1\text{H NMR}$ (300 MHz, CDCl_3): 7.13–6.80 (m, 20H, C_6H_5), 0.67 (s, 6H, CH_3). $^{13}\text{C NMR}$ (75 MHz, CDCl_3): δ 151.18, 143.87, 140.29, 139.40, 130.12, 128.87, 127.87, 127.40, 125.99, 125.50, -2.54. CV: oxidation at 1496, 1827 mV vs Ag/AgCl, reduction at -2482, -2661 mV vs Ag/AgCl. Luminescence (acetonitrile): excitation at 348 nm, emission at 466 nm.

4. Syntheses of 1,1,2,3,4,5-Hexaphenylgermacyclopentadiene (GePh) and 1,1-Dichloro-2,3,4,5-tetraphenylgermacyclopentadiene.¹³ The standard reaction sequence was followed as described above to prepare the dilithio reagent using 16.6 g of diphenylacetylene (93.3 mmol) and 646 mg of lithium wire (93.1 mmol). The dilithio reagent

(20.4 mmol, 44% yield) was quenched with 2.7 mL of germanium(IV) chloride (23 mmol) dissolved in 50 mL of diethyl ether. The red color of the dilithio reagent cleared immediately yielding a yellow solution. After 30 min of stirring, the solvent was removed in vacuo and the crude product was extracted with methylene chloride. Concentration and cooling yielded 2.76 g (5.52 mmol, 27% yield based on dilithio reagent) of yellow-green crystals of 1,1-dichloro-2,3,4,5-tetraphenylgermacyclopentadiene (no further purification was performed). A -40 °C solution of 1,1-dichloro-2,3,4,5-tetraphenylgermacyclopentadiene (247 mg, 0.494 mmol) in 10 mL of THF was quenched with phenyllithium (0.64 mL, 1.2 mmol). The ether was removed in vacuo yielding the crude germole (85% yield). GePh was purified by recrystallization from boiling absolute ethanol (10% yield based on crude).

GePh: yellow-green solid; mp 186–187 °C. Elem. Anal. Calcd for $\text{GeC}_{40}\text{H}_{30}$: C, 82.37; H, 5.18. Found: C, 82.59; H, 5.14. UV-vis ($\text{CH}_3\text{-CN}$, nm): 354 ($1.1 \times 10^4 \text{ M}^{-1}\text{cm}^{-1}$). IR (KBr, cm^{-1}): 3066 (m), 3051 (m), 3024 (m), 1594 (m), 1575 (w), 1484 (s), 1440 (m), 1431 (s), 1128 (m), 1089 (s), 1025 (m), 784 (m), 765 (m), 736 (s), 707 (s), 698 (s), 614 (m), 563 (w), 465 (m). EI-MS (70 V): major fragments at $m/z = 105, 178, 279, 357, 538$, and molecular ion at $m/z = 584$. $^1\text{H NMR}$ (300 MHz, CDCl_3): δ 7.61–7.34 (m, 10H, C_6H_5), 7.03–6.87 (m, 20H, C_6H_5). $^{13}\text{C NMR}$ (75 MHz, CDCl_3): δ 153.62, 141.14, 139.98, 139.24, 135.17, 134.87, 130.14, 129.47, 129.19, 128.60, 127.79, 127.47, 126.22, 125.70. CV: oxidation at 1495 mV vs Ag/AgCl, reduction at -1962, -2187, -2668 mV vs Ag/AgCl. Luminescence (acetonitrile): excitation at 359 nm, emission at 486 nm.

1,1-Dichloro-2,3,4,5-tetraphenylgermacyclopentadiene: yellow-green solid; mp 193 °C. UV-vis (CH_3CN , nm): 199, 296, 370. IR (KBr, cm^{-1}): 3080 (m), 3059 (m), 3023 (m), 1595 (w), 1574 (w), 1488 (s), 1441 (s), 1074 (m), 1026 (m), 912 (w), 784 (s), 763 (m), 759 (m), 740 (w), 707 (s), 695 (s), 569 (m), 414 (s). EI-MS (70 V): major fragments at $m/z = 178, 356$, and molecular ion at $m/z = 500$. $^1\text{H NMR}$ (300 MHz, CDCl_3): 7.20–7.04 (m, 16H, C_6H_5), 6.88–6.83 (m, 4H, C_6H_5). $^{13}\text{C NMR}$ (75 MHz, CDCl_3): δ 149.99, 136.61, 134.69, 132.77, 129.54, 129.52, 128.36, 128.06, 127.68, 127.47.

5. Synthesis of 1,1-Dimethyl-2,3,4,5-tetraphenylstannacyclopentadiene (SnMe).^{3,14} The standard reaction sequence was followed as described above to prepare the dilithio reagent using 20.1 g of diphenylacetylene (114 mmol) and 792 mg of lithium wire (114 mmol). A portion of the dilithio reagent solution (134 mL, 9.90 mmol) was quenched with 11.1 g of dimethyltin dichloride (50.5 mmol) dissolved in 60 mL of THF. Upon addition, the color of the dilithio reagent changed to an orange-amber color. The reaction mixture was stirred at room temperature overnight. The solvent was removed in vacuo and the residue was washed with 3×60 mL of ethanol to remove lithium chloride and unreacted tin halides, yielding 3.07 g (6.08 mmol) of SnMe (61% yield based on dilithio reagent). The crude product was purified by recrystallization from ethanol/methylene chloride (31% yield based on crude).

SnMe: pale yellow solid; mp 185–187 °C. Elem. Anal. Calcd for $\text{SnC}_{30}\text{H}_{26}$: C, 71.31; H, 5.19. Found: C, 71.11; H, 5.05. UV-vis ($\text{CH}_3\text{-CN}$, nm): 350 ($1.1 \times 10^4 \text{ M}^{-1}\text{cm}^{-1}$). IR (KBr, cm^{-1}): 3073 (m), 3049 (m), 3018 (m), 2990 (w), 2921 (w), 1594 (m), 1570 (w), 1484 (m), 1438 (m), 1280 (w), 1267 (w), 1072 (m), 1027 (m), 909 (w), 783 (m), 755 (w), 729 (w), 698 (s), 556 (m), 523 (m). EI-MS (70 V): major fragments at $m/z = 135, 178, 356$, and molecular ion at $m/z = 506$. $^1\text{H NMR}$ (300 MHz, CDCl_3): 7.10–6.76 (m, 25H, C_6H_5), 0.62 (s, $J_{\text{SnH}} = 29, 28$ Hz, 6H, CH_3). $^{13}\text{C NMR}$ (75 MHz, CDCl_3): δ 153.57 ($^2J_{\text{SnC}} = 41$), 144.91 ($^1J_{\text{SnC}} = 209, 199$ Hz), 143.02 ($^2J_{\text{SnC}} = 23$ Hz), 140.76 ($^3J_{\text{SnC}} = 32$ Hz), 130.25, 128.85 ($^3J_{\text{SnC}} = 10$ Hz), 127.77, 127.19, 125.59, 124.99, -7.75 ($^1J_{\text{SnC}} = 166, 159$ Hz). CV: oxidation at 1191, 1510 mV vs Ag/AgCl, reduction at -2197 mV vs Ag/AgCl. Luminescence (acetonitrile): excitation at 350 nm, no emission.

6. Synthesis of 1,1,2,3,4,5-Hexaphenylstannacyclopentadiene (SnPh).¹ The standard reaction sequence was followed as described above using 8.98 g of diphenylacetylene (50.4 mmol) and 350 mg of lithium wire (50. mmol). The dilithio reagent was quenched with 8.47 g of

(13) Curtis, M. D. *J. Am. Chem. Soc.* **1969**, *91*, 6011.

(14) Gustavson, W. A.; Principe, L. M.; Min Rhee, W.-Z.; Zuckerman, J. *J. Am. Chem. Soc.* **1981**, *103*, 4126.

diphenyltin dichloride (24.6 mmol) dissolved in 50 mL of diethyl ether. The reaction solution was refluxed for 0.5 h, during which time the solution became bright yellow. The solvents were removed and the residue was extracted with methylene chloride. A portion of the crude stannole (5.4 g, 32 wt %) was purified by column chromatography using petroleum ether/methylene chloride as the eluant. Further purification by recrystallization from boiling ethanol yielded 1.22 g of SnPh (2.0 mmol, 23% yield based on the crude stannole portion that was purified by column chromatography).

SnPh: yellow-green solid; mp 172–173 °C. Elem. Anal. Calcd for $\text{SnC}_{40}\text{H}_{30}$: C, 76.33; H, 4.80. Found: C, 76.40; H, 4.72. UV-vis ($\text{CH}_3\text{-CN}$, nm): 355 ($9.5 \times 10^3 \text{ M}^{-1}\text{cm}^{-1}$). IR (KBr, cm^{-1}): 3075 (m), 3056 (m), 3014 (m), 1594 (m), 1577 (w), 1481 (m), 1440 (m), 1430 (s), 1071 (m), 1021 (m), 787 (w), 779 (m), 764 (s), 741 (w), 729 (s), 699 (s), 555 (m). EI-MS (70 V): major fragments at $m/z = 120, 178, 197, 356$, and molecular ion at $m/z = 630$. ^1H NMR (300 MHz, CDCl_3): δ 7.60–7.38 (m, 10H, C_6H_5), 7.04–6.82 (m, 20H, C_6H_5). ^{13}C NMR (75 MHz, CDCl_3): δ 155.14 ($^2J_{\text{SnC}} = 45, 43 \text{ Hz}$), 142.76 ($^1J_{\text{SnC}} = 223, 213 \text{ Hz}$), 142.31 ($^2J_{\text{SnC}} = 22 \text{ Hz}$), 140.56 ($^3J_{\text{SnC}} = 32 \text{ Hz}$), 138.04 ($^1J_{\text{SnC}} = 257, 246 \text{ Hz}$), 137.14 ($^2J_{\text{SnC}} = 20 \text{ Hz}$), 130.28, 129.43 ($^4J_{\text{SnC}} = 6 \text{ Hz}$), 129.30 ($^3J_{\text{SnC}} = 11 \text{ Hz}$), 128.95 ($^3J_{\text{SnC}} = 42 \text{ Hz}$), 127.88, 127.37, 125.90, 125.37. CV: oxidation at 1539 mV vs Ag/AgCl, reduction at –2142, –2398 mV vs Ag/AgCl. Luminescence (acetonitrile): excitation at 355 nm, emission at 494 nm.

7. Synthesis of (1,2,3,4-Tetraphenylbuta-1,3-dienyl)dimethyltin Chloride.¹⁴ If a hydrolytic workup is performed for the preparation of SnMe, hydrolysis of the dimethyltin dichloride starting material can generate HCl, which reacts with SnMe yielding the ring-opened product, (1,2,3,4-tetraphenylbuta-1,3-dienyl)dimethyltin chloride. This byproduct was purified by column chromatography and recrystallization from 2-propanol (34% yield).

(1,2,3,4-Tetraphenylbuta-1,3-dienyl)dimethyltin chloride: white solid; mp 188 °C. UV-vis (CH_3CN , nm): 284 ($1.5 \times 10^4 \text{ M}^{-1}\text{cm}^{-1}$). IR (KBr, cm^{-1}): 3079 (m), 3057 (m), 3018 (m), 2919 (w), 2796 (w), 1595 (m), 1583 (w), 1571 (w), 1487 (s), 1441 (s), 1156 (w), 1077 (m), 1027 (m), 919 (m), 786 (s), 759 (s), 730 (s), 697 (s), 659 (m), 552 (s), 528 (s), 512 (s). ^1H NMR (300 MHz, CDCl_3): 7.26–6.90 (m, 23H, C_6H_5), 0.69 (s, $J_{\text{SnH}} = 30, 28 \text{ Hz}$, 6H, CH_3). ^{13}C NMR (75 MHz, CDCl_3): δ 156.96 ($J_{\text{SnC}} = 24 \text{ Hz}$), 148.11 ($J_{\text{SnC}} = 20 \text{ Hz}$), 147.41 ($^1J_{\text{SnC}} = 284, 272 \text{ Hz}$), 141.28 ($J_{\text{SnC}} = 16 \text{ Hz}$), 138.32 ($J_{\text{SnC}} = 34 \text{ Hz}$), 136.93, 135.18, 129.94, 129.81, 129.77, 129.72, 129.31 ($J_{\text{SnC}} = 11 \text{ Hz}$), 128.29, 128.27, 128.08, 127.97, 127.58 ($J_{\text{SnC}} = 3 \text{ Hz}$), 127.25, 126.74, 125.97 ($J_{\text{SnC}} = 5 \text{ Hz}$), 1.56 ($^1J_{\text{SnC}} = 192, 201 \text{ Hz}$). CV: oxidation at 1450, 1750 mV vs Ag/AgCl, reduction at –2250 mV vs Ag/AgCl. Luminescence (acetonitrile): excitation at 284 nm, emission at 391 nm.

8. Synthesis of (E,E)-1,2,3,4-Tetraphenylbuta-1,3-diene.⁷ If the dilithio reagent is hydrolyzed, (E,E)-1,2,3,4-tetraphenylbuta-1,3-diene can be isolated by column chromatography and purified by recrystallization from 2-propanol (77% yield).

(E,E)-1,2,3,4-Tetraphenylbuta-1,3-diene: white solid; mp 188 °C. UV-vis (CH_3CN , nm): 327, 316. IR (KBr, cm^{-1}): 3099 (w), 3078 (m), 3059 (m), 3020 (m), 2996 (w), 2926 (w), 1596 (m), 1488 (s), 1441 (s), 1070 (m), 1026 (m), 927 (m), 917 (m), 867 (m), 783 (s), 763 (s), 753 (s), 702 (s), 691 (s). ^1H NMR (300 MHz, CDCl_3): 7.44–7.34 (m, 5H, C_6H_5), 7.06–7.04 (m, 3H, C_6H_5), 6.80–6.76 (m, 2H, C_6H_5), 6.35 (s, 1H, CH). ^{13}C NMR (75 MHz, CDCl_3): δ 145.58, 139.75, 137.23, 131.64, 130.38, 129.46, 128.79, 127.79, 127.33, 126.59.

C. Spectroscopic, Electrochemical, and Elemental Analyses. 1. UV-visible absorption spectra were recorded as acetonitrile solutions with a Perkin-Elmer Lambda 20 Spectrophotometer operating in double-beam mode with a solvent blank as the reference cell.

2. Luminescence spectra were recorded on an SLM-Aminco AB-2 spectrofluorometer. Corrected spectra are recorded in all cases.

3. Infrared spectra were recorded in a KBr matrix on either a Nicolet Model 205 or a BioRad FTS-7.

4. Electron impact mass spectra were obtained on a Hewlett-Packard 5988A mass spectrometer operating at 70 V with a source temperature of 250 °C. All samples were introduced using a direct insertion probe. For all metalloles, the distribution and abundance of molecular ion peaks exactly matched those predicted based on the isotopic abundances of the constituent elements. The most abundant

molecular ion peak and the major fragments are tabulated in the Experimental Section.

5. NMR Spectroscopy. ^1H NMR spectra were recorded in CDCl_3 (99.9%, Aldrich) on either a Bruker AC-P 300 or a Bruker MSL300 NMR spectrometer. Residual chloroform was used as the internal standard (7.25 ppm). ^{13}C NMR were similarly recorded at 75 MHz using CDCl_3 as the internal standard (77.00 ppm). ^{13}C NMR spectra with tin satellites were obtained by repetitive scanning (between 16 000 and 40 000 scans). Acquisition parameters are available from the authors.

6. Electrochemical analyses were performed on a Bioanalytical Systems CV-50W System operating in cyclic voltammetry mode. A three-electrode system consisting of platinum working and auxiliary electrodes and a Ag/AgCl reference electrode was used. Tetra-*n*-butylammonium hexafluorophosphate (Aldrich) was used as a supporting electrolyte in all cases. The standard scan rate was 100 mV/s. Reduction cyclic voltammograms were recorded from 0 to –3.200 V vs Ag/AgCl in tetrahydrofuran solutions, and oxidation voltammograms were recorded from 0 to +2.200 V vs Ag/AgCl in methylene chloride. Acetonitrile was not used as a solvent because preliminary experiments indicated that it was oxidized at +2.0 V and reduced at –2.2 V. All electrochemical measurements were performed using the following protocol: Solutions of tetra-*n*-butylammonium hexafluorophosphate (0.1 M), prepared with freshly distilled tetrahydrofuran (from benzophenone ketyl) or methylene chloride (distilled from phosphorus pentoxide), were transferred by syringe to the dry electrochemical cell. The solution was bubble-degassed for ca. 5 min with nitrogen and then the CV of the electrolyte solution was recorded. Next, approximately 3–5 mg of the metallole was dissolved in the solution, and it was degassed for an additional 5 min before the CV was recorded. To ensure anhydrous conditions, approximately 10 mg of activated alumina was added to each. By scavenging any water, the alumina improved the smoothness of the CV. The alumina was activated by heating to ~120 °C at < 0.01 mmHg for several days.

7. Elemental analysis of each metallole was carried out using a Perkin-Elmer 2400 Series II analyzer. No significant differences were observed, at the 95% confidence level, between theoretical expectations and actual compositions. Results are tabulated in the Experimental Section.

D. Molecular orbital calculations were performed using MacSpartan Plus, version 1.1.7, (Wavefunction, Inc.) operating on a 7600/132 Power Macintosh microcomputer. The output of the semiempirical calculations for the six metalloles, performed at the AM1 level of theory, is available in the Supporting Information.

E. X-ray Crystal Structure. Crystals of hexaphenylstannole (SnPh) were obtained by recrystallization from 2-propanol. The X-ray data were collected at room temperature using an Enraf-Nonius CAD4 diffractometer with graphite-monochromated $\text{Mo K}\alpha$ radiation ($\lambda = 0.7107 \text{ \AA}$). From the systematic absences, the space group was determined to be $P\bar{1}$. The cell parameters ($a = 10.353(2) \text{ \AA}$, $b = 16.679(2) \text{ \AA}$, $c = 9.482(1) \text{ \AA}$; $\alpha = 99.91(1)^\circ$, $\beta = 106.33(1)^\circ$, $\gamma = 77.80(1)^\circ$) were obtained by a least-squares fit of $\sin^2 \theta$ values for 25 reflections in the range $13^\circ < \theta < 17^\circ$. Integrated intensities were measured by $\omega - 2\theta$ scans with ω -scan width $(1.00 + 0.35 \tan \theta)^\circ$, using varying scan speeds determined by a prescan. Three standard reflections, (–3 0 1) (0 –3 –1) (1 1 1), were monitored every 60 min. There was no loss of intensity during the data collection. A hemisphere of data ($\sin \theta/\lambda < 0.60$; $0 \leq h \leq 12$, $-19 \leq k \leq 19$, $-11 \leq l \leq 10$) were collected, yielding a total of 5571 measured reflections, excluding standard reflections. Lorentz, polarization, and absorption corrections were applied. The absorption coefficient, $\mu = 8.73 \text{ cm}^{-1}$, gave transmission factors in the range 0.941–1.000.¹⁵ Averaging 649 symmetry related reflections gave $R_{\text{int}} = 0.032$ and resulted in 5143 independent reflections, 3491 having $F_o > 3\sigma(F_o)$.

A partial structure was found using direct methods.¹⁶ All remaining non-hydrogen atoms were found in successive difference maps after

(15) Fair, C. K. *MolEN. An Interactive Intelligent System for Crystal Analysis*; Enraf-Nonius: Delft, The Netherlands, 1990.

(16) Main, P. *MULTAN78, A system of computer programmes for the automatic solution of crystal structures from X-ray diffraction data*; Department of Physics, University of York: York, England, 1978.

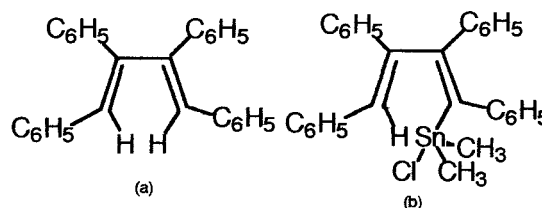
Table 1. UV–Visible Absorption Band Maxima in nm (in Acetonitrile Solution)

	methyl	phenyl
Si	351	360
Ge	348	354
Sn	350	355

refinements by differential Fourier methods.¹⁷ The positional and isotropic displacement parameters thus obtained were then used as input to a full-matrix, least-squares refinement.¹⁸ From differential Fourier maps all hydrogen atoms were located. Atomic positional, anisotropic displacement parameters for non-hydrogen atoms and isotropic displacement parameters for hydrogen atoms were varied, together with the scale factor, and converged with $\Delta/\sigma < 0.01$. The extinction correction was omitted after the extinction coefficient failed to assume a significant value.¹⁹ The quantity $\sum w||F_o| - |F_c||^2$ was minimized with weights $w = 1/\sigma^2(F_o)$ and $\sigma^2(F_o) = \sigma_{cs}^2 + (0.02F_o)^2$, where σ_{cs}^2 is the variance due to counting statistics. Atomic scattering factors were those as calculated by Cromer and Waber.²⁰ Anomalous dispersion corrections were included.²¹ Residual maxima in the final difference Fourier map were $0.5 \text{ e } \text{Å}^{-3}$ near the Sn atom. The refinement converged with fit indices $R(F_o) = 0.037$, $R_w(F_o) = 0.038$, and $S = 1.11$.

Results and Discussion

A. Photophysical Spectroscopic Properties. UV–visible absorption data obtained in acetonitrile solution are presented in Table 1. The methyl-substituted metalloles (SiMe, GeMe, and SnMe) all display a well-defined maximum near 350 nm, while the phenyl-substituted metalloles display a maximum near 358 nm. The insensitivity to heteroatom substitution implies that the absorption involves electronic transitions between molecular orbitals localized primarily on the diene and/or on the phenyl rings of the chromophore. In all cases, absorbance maxima showed no significant sensitivity to changes in solvent polarity.²² Two byproducts were isolated during the course of this research (Figure 3); (*E,E*)-1,2,3,4-tetraphenylbutadiene (the hydrolysis product of the dilithio reagent) and (1,2,3,4-tetraphenylbuta-1,3-dienyl)dimethyltin chloride (the product of HCl addition to an Sn–Cl bond), are both white solids with no appreciable absorption at 350 nm, confirming the role of the metallole in the chromophore. Luminescence data are presented in Table 2. The luminescence properties of these metalloles have been briefly noted in the literature.^{6,7} In contrast to the absorption data, the luminescence of the methyl-substituted compounds shows a strong dependence on the nature of the heteroatom (Table 2). The SiMe compound has a featureless band with an emission maximum at 480 nm, GeMe shows a higher energy luminescence band at 466 nm, and SnMe fails to luminesce. The same dependence on the heteroatom was not observed for the corresponding phenyl-substituted compounds, which all showed a featureless luminescence band near 490 nm.²³

**Figure 3.** Structures of two byproducts of this research: (a) (*E,E*)-1,2,3,4-tetraphenylbutadiene and (b) (1,2,3,4-tetraphenylbuta-1,3-dienyl)dimethyltin chloride.**Table 2.** Luminescence Band Maxima in nm (in Acetonitrile Solution)^a

	methyl	phenyl
Si	480	496
Ge	466	486
Sn	none	494

^a Excitations at UV–vis band maxima.

Table 3. Anodic and Cathodic Peak Potentials (mV) for the Irreversible Oxidation and Reduction of Metalloles in Solution

	oxidation	reduction
SiMe	1482	–2174
GeMe	1496	–2482
SnMe	1191	–2197
SiPh	1527	–1943
GePh	1495	–1962
SnPh	1539	–2142

The simplest explanation for this heteroatom dependence relates to the electron density associated with the heteroatom and the ability of the substituents (not the chromophore) to absorb electron density. When the substituents are phenyl groups, they have a large capacity to absorb and buffer any electron density pushed off the heteroatom.

B. Electrochemical Properties. The electrochemical properties of the six metalloles were studied in order to determine if their redox behavior could elucidate the reason for the lack of luminescence in SnMe. Although several of the compounds have been known to undergo a two-electron reduction by alkali metals, and spectroscopic properties of the reduced state of SiMe have been reported,^{24,25} thorough electrochemical characterization of the compounds has been lacking. Table 3 summarizes the data obtained from cyclic voltammetry experiments. In cases where multiple waves were observed, only the first potential is tabulated. For SiMe, GeMe, and SnMe, the oxidative and reductive cyclic voltammograms, in methylene chloride and tetrahydrofuran, respectively, are shown in Figure 4.

Each compound exhibited at least one irreversible reduction wave and two irreversible oxidation waves. The peak potentials of the phenyl-substituted compounds showed little dependence on the heteroatom. In the methyl series, two interesting anomalies are observed. GeMe is the most difficult of the six compounds to reduce, with a reduction potential some 300 mV more negative than those of the other five metalloles. This is consistent with the observation that the luminescence emission from GeMe occurs at higher energy than that of any of the other compounds.

An even more interesting observation is made in the case of SnMe. Comparison of the oxidation potentials of the series indicates that SnMe is the easiest of the compounds to oxidize.

(17) Sheldrick, G. M. *SHELX-76, Program for Crystal Structure Determination*; University of Cambridge: Cambridge, England, 1976.

(18) Craven, B. M.; Weber, H.-P.; He, X. M. *The POP Least-Squares Refinement Procedure*; University of Pittsburgh: Pittsburgh, PA, 1987.

(19) Becker, P. J.; Coppens, P. *Acta Crystallogr., Sect. A* **1974**, *30*, 129–147.

(20) Cromer, D. T.; Waber, J. T. *International Tables for X-ray Crystallography*; Kynoch Press: Birmingham, England, 1974; Vol. IV, pp 71–147 (present distributor Reidel: Dordrecht).

(21) Cromer, D. T.; Waber, J. T. *International Tables for X-ray Crystallography*; Kynoch Press: Birmingham, England, 1974; Vol. IV, pp 148–151.

(22) Toluene, methylene chloride, dimethyl formamide, acetonitrile, and methanol were used.

(23) For all compounds studied, the luminescence band maxima are not affected by a change in solvent. Solvents of greatly different polarity lead to essentially identical luminescence spectra.

(24) Janzen, E. G.; Pickett, J. B.; Atwell, W. H. *J. Organomet. Chem.* **1967**, *10*, P6.

(25) Janzen, E. G.; Harrison, W. B.; DuBose, C. M., Jr. *J. Organomet. Chem.* **1972**, *40*, 281.

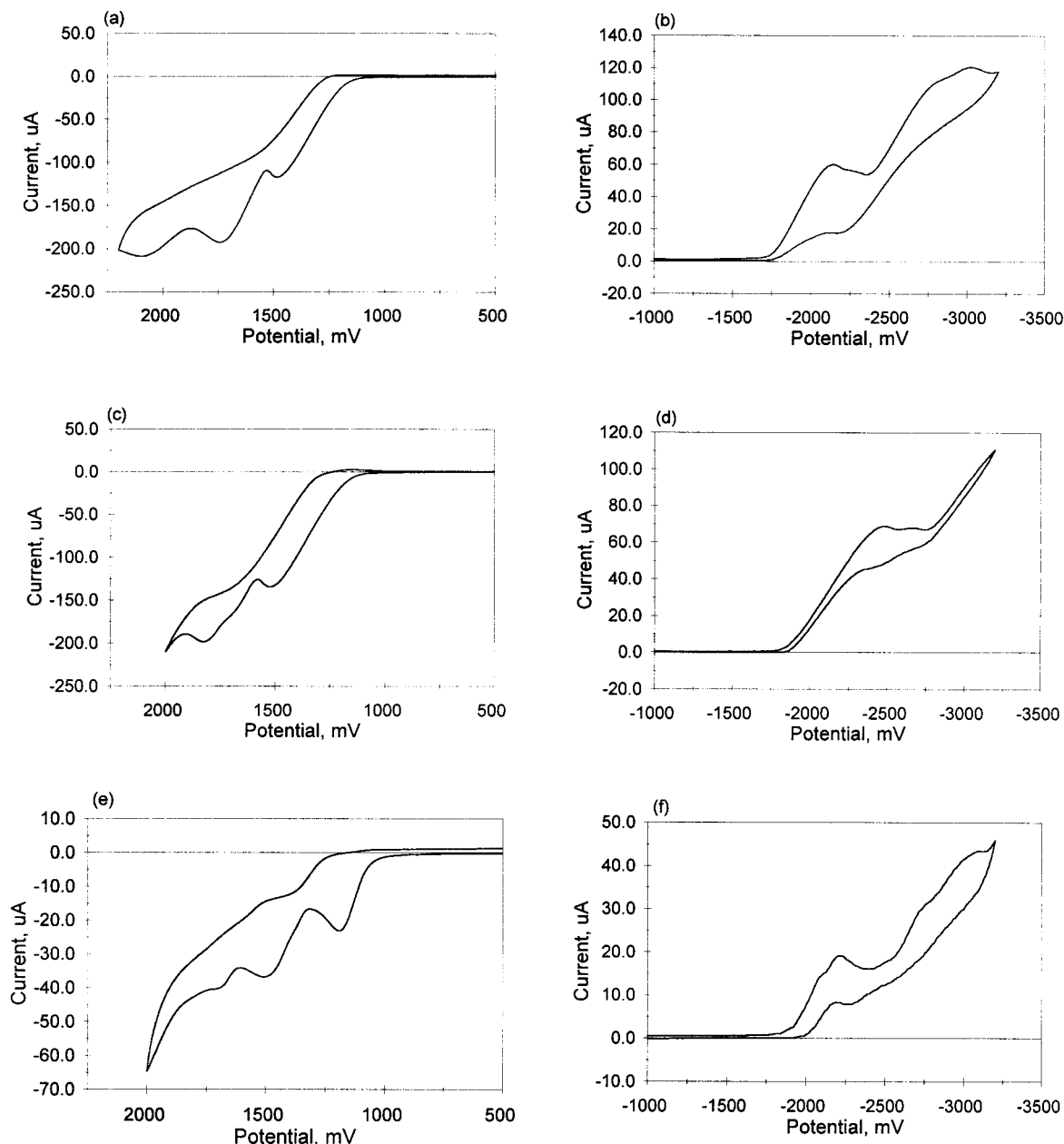


Figure 4. Cyclic voltammograms of methylmetalloles: (a) SiMe oxidation, (b) SiMe reduction, (c) GeMe oxidation, (d) GeMe reduction, (e) SnMe oxidation, and (f) SnMe reduction.

Its oxidation peak potential is almost 300 mV less positive than the other compounds, indicating a HOMO of significantly higher energy than those of SiMe or GeMe. The isopotential surface of the LUMO of SnMe has appreciable density on Sn, whereas the LUMOs of SiMe and GeMe have no density at the metals (the same trend is seen in the LUMOs of SiPh, GePh, and SnPh). The relative ease of oxidation of SnMe also may be an indication of relatively diffuse electron density on Sn, consistent with the fact that of the three heteroatoms, Sn has the smallest electronegativity and largest size. This observation also is consistent with the observation that the carbons of the methyl substituents of SnMe are the most shielded of the carbons attached directly to the heteroatom in all the metalloles. The electron density on Sn in SnMe results in such perturbations to the chromophore that the compound does not luminesce. In SnPh, the phenyl substituents on the heteroatom are not shielded to the extent that the methyl substituents are, indicating that the phenyl substituents are able to absorb electron density from the

heteroatom more effectively than the methyl substituents, attenuating the perturbations to the chromophore.

C. NMR Spectroscopy. The ^{13}C NMR data of the series provide insight into the anomalous luminescence behavior of SnMe. The chemical shifts of the six metalloles are tabulated in Table 4; J_{SnC} values are included when detected.²⁶ The spectra indicate that the molecules possess C_{2v} symmetry in solution with a plane of symmetry bisecting the C2–C3 bond and passing through the heteroatom. (See Figure 6 for the carbon numbering scheme. For the methyl series, the two phenyl substituents, C51–C56 and C61–C66, are replaced with two methyl carbons, C5 and C6.)

The resonances for the C2 and C3 carbons are the most deshielded in the ^{13}C NMR spectra of the six metalloles, lying significantly farther downfield than any other resonance. The

(26) The presence of two NMR-active isotopes of tin (^{119}Sn , 8.58% and ^{117}Sn , 7.61%) provide unequivocal assignments of the carbon resonances in the ^{13}C NMR spectra of SnMe and SnPh.

Table 4. ^{13}C NMR Chemical Shifts of the Six Metalloles (Sn–C Coupling, in Hz, Presented in Parentheses if Detected)

	C2, C3	C1, C4	C11, C41	C21, C31	C51, C61	C5, C6	C12,16,...,C46	C22,26,...,C36	C13,15,...,C45	C23,25,...,C35	C14,44	C24,34	C52,56,...,C66	C53,55,...,C65	C54,64
SiMe	153.90	141.80	139.80	138.80		-3.90	128.80	130.00	127.40	127.90	125.50	126.20			
SiPh	156.70	139.56	139.50	138.80	131.60		129.20	130.00	127.70	128.20	125.60	126.40		127.40	130.10
GeMe	151.20	143.90	140.30	139.40		-2.54	128.90	130.10	127.40	127.90	125.50	126.00			
GePh	153.60	141.10	140.00	139.20	134.90		129.20	130.10	127.80	128.60	125.70	126.20		127.50	129.50
SnMe	153.57 (41) ^a	144.91 (209, 199) ^b	143.02 (23) ^a	140.76 (32) ^a		-7.75 (166, 159) ^b	128.85 (10) ^a	130.25	127.19	127.77	124.99	125.59		127.50	
SnPh	155.14 (45, 43) ^a	142.76 (223, 213) ^b	142.31 (22) ^a	140.56 (32) ^a	138.04 (257, 246) ^b		129.30 (11) ^a	130.28	127.37	127.88	125.37	125.90 (20) ^a	137.14	128.95 (42) ^a	129.43 (6)

^a $^2J_{\text{SnC}}$, ^b $^1J_{\text{SnC}}$, ^c $^3J_{\text{SnC}}$.

broad-band decoupled ^{13}C NMR spectrum of the aromatic region of SnPh, shown in Figure 5, is representative. Although one might expect the C1 and C4 resonances to be the most deshielded, this is not the case.²⁷ The assignments of the C2 and C3 carbon resonances were made by J_{SnC} value observations, which have been extensively documented in the literature, and comparison of the spectra of the six metalloles (Table 4).^{28–31} The chemical shift of the C2 and C3 resonances of the germoles are the most shielded with respect to the siloles and stannoles.

In the phenyl series, the C51 and C61 resonances become increasingly deshielded as the atomic number of the heteroatom increases. However, in the methyl series this trend is observed only from silicon to germanium; the C5 and C6 resonances of SnMe are the most shielded, consistent with the anomalies noted in the luminescence properties and the electrochemical data of the six metalloles.

D. Infrared Spectroscopy. The infrared spectra of all the metalloles are predictably similar. Antisymmetric and symmetric aromatic C–H stretching absorption bands occur between 3080 and 3014 cm^{-1} for all the metalloles. All six metalloles display $\nu(\text{C}=\text{C})$ at $1595 \pm 1 \text{ cm}^{-1}$ and $1574 \pm 4 \text{ cm}^{-1}$. An out-of-plane skeletal mode absorption band of the monosubstituted aromatic rings at 695–700 cm^{-1} is present in all the spectra.³² The largest differences in the infrared spectra are the presence of aliphatic $\nu(\text{C}-\text{H})$ stretch bands in the methyl series. The antisymmetric and symmetric methyl $\nu(\text{C}-\text{H})$ stretches both move to higher wavenumber as the mass of the metal increases; 2958 and 2898 cm^{-1} for SiMe, 2976 and 2906 cm^{-1} for GeMe, and 2990 and 2921 cm^{-1} for SnMe.

E. Molecular Structure. An ORTEP diagram of the X-ray crystal structure of the hexaphenylstannole (SnPh) is shown in Figure 6.³³ (Structural parameters are listed in Table 5. Atomic coordinate files are available in the Supporting Information.) This structure contains an unusual finding: one of the phenyl groups (C11, C12, ..., C16 in Figure 6) is practically coplanar with the metallole ring (Sn, C1, C2, C3, C4). (The torsion angle Sn–C1–C11–C12 is 1.2(6)°.) This is most probably attributable to crystal packing forces, and it certainly is not indicative of the structure in solution, which we know to possess C_{2v} symmetry on average. There are no short intramolecular distances (the shortest being 2.53 Å for H13...H52).

F. Molecular Orbital Calculations. For all six metalloles, equilibrium geometries were obtained at the AM1 semiempirical level of theory using MacSpartan Plus, version 1.1.7, on a Power Macintosh 7600/132. Starting geometries were obtained using the SYBYL force field after assembling the molecule in the MacSpartan graphical user interface.

- (27) CNMR Predictor, a ^{13}C NMR simulator program (Advanced Chemistry Development Inc., Toronto, Ontario, Canada), predicted the C1 carbons to be most downfield in the spectra of the germoles and the stannoles; personal communication from Kathleen Gallagher, Instrumentation Center, University of New Hampshire.
- (28) See: Wrackmeyer, B. In *Annual Reports on NMR Spectroscopy*; Webb, G. A., Ed.; Academic Press: London, 1985; Vol. 16, pp 73–186 and references therein.
- (29) Bullpitt, M.; Kitching, W.; Adock, W.; Doddrell, D. *J. Organomet. Chem.* **1976**, *116*, 161.
- (30) Doddrell, D.; Burfitt, I.; Kitching, W.; Bullpitt, M.; Lee, C.-H.; Mynott, R. J.; Considine, J. L.; Kuivila, H. G.; Sarma, R. H. *J. Am. Chem. Soc.* **1974**, *96*, 1640.
- (31) Mitchell, T. N.; Podesta, J. C.; Ayala, A.; Chopra, A. B. *Magn. Reson. Chem.* **1988**, *26*, 497.
- (32) Bellamy, L. J. In *The Infrared Spectra of Complex Molecules*, 3rd ed.; Chapman and Hall: London, 1975; p 87.
- (33) Johnson, C. K. ORTEP-II, Report ORNL-5138, Oak Ridge National Laboratory, TN, 1976.

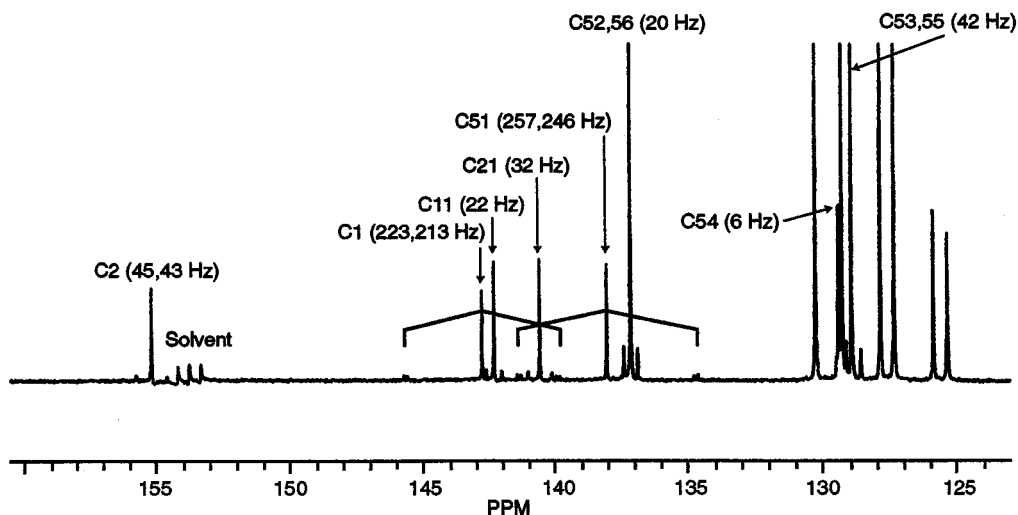


Figure 5. Aromatic region of the ^{13}C NMR spectrum of hexaphenylstannole (SnPh). Coupling to $^{119/117}\text{Sn}$ is clearly visible for the six carbon atoms below 135 ppm. Note that the furthest downfield resonance (C2), 155.14 ppm, has a much smaller coupling than either the 142.76 ppm resonance (C1) or the 138.04 ppm resonance (C51).

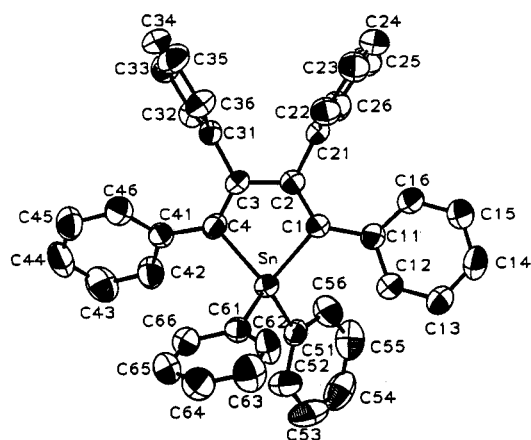


Figure 6. ORTEP diagram of hexaphenylstannole (SnPh). Thermal ellipsoids are at the 50% probability level. Hydrogens are omitted for clarity.

Pertinent geometrical parameters are summarized in Table 6 along with internuclear distances obtained from X-ray diffraction studies of crystal structures. For all structures, geometric optimization was performed at the AM1 level, followed by single energy point calculations also at the AM1 level. For each metallole, Mulliken charges for all atoms present in the molecule were generated. (See Supporting Information for tables of Mulliken charges for each metallole.) In every case the charge on C2 was considerably more positive than the charge on C1. These results are consistent with the ^{13}C NMR resonance assignments, in which C2 is always downfield from C1. Molecular orbital isotopotential plots were constructed to view qualitative changes in the electronic structure of related systems upon substitution of the heteroatom. The HOMOs and LUMOs for all six compounds displayed qualitatively similar surfaces. All the HOMOs resembled the HOMO of the model compound presented in Figure 2a with A_2 symmetry under C_{2v} . Most of the HOMO surfaces had some density at the phenyl rings substituted on the diene section of the metallole. The LUMOs all resembled the model compound LUMO, Figure 2c, except for the stannoles, where the LUMOs had significant orbital density at the tin atoms.³⁴ Ab initio calculations were performed

(34) The orbital information is available upon request from the authors.

Table 5. Crystallographic Data for Hexaphenylstannole (SnPh)

formula	$\text{SnC}_{40}\text{H}_{30}$
fw	629.38 au
space group	$P\bar{1}$
Z	2
a, Å	10.353(2)
b, Å	16.679(2)
c, Å	9.482(1)
α , deg	99.91(1)
β , deg	106.33(1)
γ , deg	77.80(1)
V, Å ³	1524.8(4)
T, °C	25
λ , Å	0.7107
d(calcd), g/cm ³	1.372
Mo K α , mA, kV	20 mA, 45 kV
μ , cm ⁻¹	8.73
range of transmission factors	0.941–1.000
reflections collected	5571
R_{int}	0.032
independent reflections	5143
used in refinement:	3491 (3σ)
number of variables	490
$R(F_o)^a$	0.037
$R_w(F_o)^b$	0.038
S^c	1.11

^a $R(F_o) = \sum ||F_o| - |F_c|| / \sum |F_o|$. ^b $R_w(F_o) = (\sum w(|F_o| - |F_c|)^2 / \sum w|F_o|^2)^{1/2}$. ^c $S = (\sum w(|F_o| - |F_c|)^2 / (N_o - N_v))^{1/2}$ where N_o = the number of observed reflections and N_v = the number of variables.

on the hydrogen-substituted silole and germole at the Hartree–Fock level of theory using the Pople split-valence 3-21G* basis set. These calculations provided qualitatively similar results as the lower level of theory.

Conclusion

Taken together, the experimental measurements and theoretical studies allow a straightforward explanation of the activation–deactivation cycle of these metalloles. Absorption causes an electronic transition in the chromophore which is unaffected by heteroatom substitution. This excited state decays to an intermediate state that, in the case of the phenyl-substituted compounds, undergoes radiative decay to the ground state, emitting a photon at approximately 490 nm and showing relatively little dependence on the heteroatom.

On the basis of the results for the methyl series, it is clear that the heteroatom perturbs the electronic/vibrational structure

Table 6. Comparison of Calculated and Actual Metallole Bond Distances (Å) and Bond Angles (deg)^a

	E–C1/C4	E–C5(1)/C6(1)	C2–C3	C1(4)=C2(3)	C1–E–C4	C5(1)–E–C6(1)
SiMe						
theory	1.833	1.818	1.486	1.353	92.2	110.7
actual (ref 11)	1.868	1.855	1.511	1.358	92.7	110.2
GeMe						
theory	1.968	1.973	1.481	1.351	88.0	110.1
actual (ref 12)	1.945	1.944	1.508	1.347	89.9	110.2
SnMe	2.110	2.099	1.485	1.350	83.7	113.0
SiPh	1.842	1.777	1.485	1.354	91.9	111.6
GePh	1.965	1.944	1.482	1.351	87.8	112.1
SnPh						
theory	2.110	2.083	1.484	1.350	84.1	111.6
actual	2.126	2.125	1.511(6)	1.352	84.6(2)	112.3(2)

^a Errors associated with the actual structures (esd's) are reported for unique bond distances (C2–C3) and bond angles [C1–E–C4 and C5(1)–E–C6(1)], while the average bond distances are reported for equivalent bond lengths.

of the emissive state, resulting in the higher energy emission of GeMe and the lack of luminescence in SnMe. The perturbation of the emissive state by the heteroatom cannot be attenuated as effectively by the methyl-substituted metalloles as it apparently is by the phenyl-substituted compounds. In the extreme case of SnMe, the perturbation is so significant that a now more efficient nonradiative decay path drains the excited state more rapidly than does the radiative decay mechanism, effectively quenching the luminescence.

Acknowledgment. Work at Brookhaven National Laboratory was carried out under Contract DE-AC02-98CH10886 with the U.S. Department of Energy, Office of Basic Energy Sciences. Special thanks to Kathleen Gallagher and Drs. David Ofer, Peter Trumper, and Elizabeth Stemmler for thoughtful discussions and assistance. All synthetic work was carried out at the University

of Southern Maine and supported by the USM Chemistry Department and the USM Office of the Dean of the College of Arts and Sciences. We are also grateful to the Chemistry Department at Bowdoin College, Brunswick, ME, for the use of their NMR and mass spectrometers.

Supporting Information Available: Tables of crystal data and structural refinement, atomic coordinates and equivalent isotropic displacement parameters, complete bond lengths and angles, anisotropic displacement parameters, and hydrogen coordinates and isotropic displacement parameters for SnPh and output of MacSpartan semiempirical molecular orbitals calculations including Cartesian coordinates and Mulliken charges for each metallole. This material is available free of charge via the Internet at <http://pubs.acs.org>.

IC980662D